Exploring the role of differential gene expression in the age-associated impairment of peripheral nerve regeneration

Honors Thesis
Presented to the College of Arts and Sciences
Cornell University
in Partial Fulfillment of the Requirements for the
Biological Sciences Honors Program

by
Kareena Sagar
May 2020
Supervisor: Dr. Jonathan Cheetham

ABSTRACT

The peripheral nervous system's ability to regenerate after injury declines with age, but the reason for why this occurs is unknown. With the goal to understand the role of age-associated transcriptional changes in the impairment of peripheral nerve injury, I conducted a differential gene expression experiment using RNA sequencing and functional recovery experiments with gait analysis and peak tetanic force measurements. In young mice, genes involved in cell proliferation and neurogenesis were upregulated compared to old mice. In contrast, in aged mice I observed upregulation of genes encoding proteinases and pro-inflammatory cytokines. Following a peripheral nerve injury, young animals and old animals expressed a similar ability to activate regenerative transcriptional programs. Gait analyses and measurements of muscle strength showed no significant difference nor any delay in the ability of old animals to recover from peripheral nerve injury. In summary, this study identified several markers of inflammatory and immune system pathways and pathways involved in nerve regeneration that differ in their expression between young and old mice. Understanding the role of these pathways in nerve regeneration may provide therapeutic targets to enhance regeneration in aging individuals.

INTRODUCTION

Although previous studies have established a delay in the functional recovery in old animals after peripheral nerve injury and have identified some of the important genes in the repair pathway, they have not determined how the transcriptional profile of macrophages and immune cells after peripheral nerve injury is different between young and old animals. I sought to understand how macrophages from wild-type mice alter their gene expression after sciatic nerve injury by harvesting the regenerative bridges from conduits and isolating the macrophages using flow cytometry.

In comparison to the limited regenerative capacities observed in the central nervous system (CNS), the peripheral nervous system (PNS) has marked capabilities for repair (Huebner & Strittmatter, 2009). In mammals, this process is sufficient to restore some motor and sensory function after peripheral nerve trauma, but the ability to do so declines with age (Painter et al., 2014; Pestronk, Drachman, & Griffin, 1980; Tanaka & Webster, 1991; Vaughan, 1992; Verdú, Ceballos, Vilches, & Navarro, 2000). Disorders and disease due to nerve degeneration or incomplete regeneration include both movement disorders and sensory disorders such as hearing and balance loss and pain syndromes (Verdú et al., 2000). The decline in repair with aging is therefore particularly problematic in an aging population. It is estimated that 1 in 3 people over the age of 65 suffer from some form of peripheral nerve neuropathy that causes these disabling conditions (Cho, Mold, & Roberts, 2006). Due to the extent, and potentially disabling effects, of peripheral nerve injury in all age groups, the clinical significance of understanding peripheral nerve repair is paramount.

Regeneration of the PNS after injury requires successful coordination and control of a symphony of complex systems. After a peripheral nerve injury (PNI), neurons must make the

transformation from generating action potentials to supporting repair and regrowth. This process depends on the peripheral neuron's capacity to activate the repair pathway, as well as on the extracellular matrix and extrinsic factors within the neuron's environment, including macrophages and Schwann cells (SC) (Chen, Yu, & Strickland, 2007; Painter et al., 2014). Soon after injury, Schwann cells in the distal nerve stump of the axon are dedifferentiated to express a repair phenotype (Fu & Gordon, 1997; Stratton et al., 2016; Ydens et al., 2012). In the first three days after injury, these re-programmed Schwann cells remove axonal fractions and myelin from the injury, secrete pro-regenerative factors, and recruit macrophages to the injury site that help complete the removal of debris (A. L. Cattin & Lloyd, 2016; Gomez-Sanchez et al., 2015). Macrophages also induce expression of both Vascular Endothelial Growth Factor (VEGF-A) (A.-L. Cattin et al., 2015) and Nerve Growth Factor (NGF) (Lindholm, Hengerer, Zafra, & Thoenen, 1990) which promote angiogenesis and axonal growth, making them important in both the inflammatory and regenerative process (Gaudet, Popovich, & Ramer, 2011; Lindholm, Heumann, Meyer, & Thoenen, 1987; Taskinen & Röyttä, 1997). Among the factors thought to be involved in neuronal growth are trophic factors such as neurotrophins, cytokines, insulin-like growth factors (IGFs), and glial-cell-line-derived neurotrophic factors (GDNFs) (Araki, Nagarajan, & Milbrandt, 2001; Fu & Gordon, 1997; Painter et al., 2014; Scheib & Höke, 2016). In addition, the immediate early gene, c-Jun, has been implicated in the regulation of the SC repair phenotype (Painter et al., 2014). These data suggest that axonal regrowth, and subsequently functional recovery, are dependent on the host immune response to nerve injury and ability to adjust expression levels of genes related to cell viability, proliferation, differentiation, regeneration, and myelination (J.-H. Liu et al., 2018).

Previous studies exploring the mechanisms underlying peripheral nerve regeneration have cited a reduction or delay in the ability of aged animals to recover full sensory and motor function after peripheral nerve injury (Painter et al., 2014; Scheib & Höke, 2016; Vaughan, 1992; Verdú et al., 2000). Transcriptional profiling revealed age-related differences in genes pertaining to the cell cycle, DNA replication, and the extracellular matrix, with increased expression in younger animals indicating that they have an increased capacity for cell proliferation (Painter et al., 2014; Verdú et al., 2000). In addition to these changes, there have been reports of fewer macrophage markers indicating less success in recruiting macrophages to the injury site, a muted cytokine response, and a decreased density of regenerating axons in aged animals (Scheib & Höke, 2016; Verdú et al., 2000). Additionally, a markedly higher level of expression of immediate early genes has been observed, especially in an initial burst one day after injury (Painter et al., 2014). This may correlate to a delay in the function of repair-programmed Schwann cells, with a slower rate of Wallerian degeneration and macrophage recruitment in older mice. These studies suggest that some transcriptional differences between young and old animals could lead to downstream effects in the peripheral nerve regeneration pathway, especially in relation to the dedifferentiation of Schwann cells and to macrophage phenotypes that influence the ability to regenerate.

Since neuromuscular diseases produce characteristic changes in gait in humans and animals, gait analysis can be used to measure the degree of motor recovery after peripheral nerve injury. A single gait cycle consists of a stance phase when the foot is in contact with the ground and a swing phase when the foot is off the ground (Yu, Matloub, Sanger, & Narini, 2001). Tracking the angles between joints can provide insight in how the muscle is reinnervated after injury. Hock angle, for example, is the angle formed by the intersection of lines extending from the stifle to the hock and from the hock to the metatarsal head. Following injury, denervation results in loss of

neuronal control of muscle movement and subsequent muscle atrophy. As a result, the hock angle of an injured leg during mid-stance will be less than that of an uninjured leg (Lin, Pan, Horn, Sabbahi, & Shenaq, 1996). This parameter can track recovery of the injured leg after a nerve injury.

As previously mentioned, muscle atrophy follows injury denervation. While some muscle mass is regained with reinnervation, residual weakness after nerve repair is a common issue in rehabilitation (Mackinnon & Dellon, 1988). Measuring the force of peak tetanic muscle contraction can be a useful tool in evaluating muscle strength after nerve injury and repair (Sobotka & Mu, 2010; Yoshimura, Asato, Cederna, Urbanchek, & Kuzon, 1999). Muscle fiber-type composition, fiber length, cross-sectional area, and velocity of shortening all contribute to muscle power production, making power production a valid indication of the muscle's mechanical function (Yoshimura et al., 1999).

In this study, gait analysis, peak tetanic force measurements of the gastrocnemius muscle, and gastrocnemius muscle weights are used to compare degree and rate of motor recovery in young and old mice after a left tibial nerve injury. To determine if changes in macrophage phenotype are likely to contribute to the reduced regenerative capacity in older animals, I performed RNA sequencing of macrophages from regenerative post-sciatic nerve injury bridges to provide insight on differentially expressed genes between young and old mice. RNA sequencing concentrates all RNA in cells to profile levels of transcripts, providing insight on which genes are active and the downstream pathways these active genes may impact (Wang, Gerstein, & Snyder, 2009). This may provide us information on the impediments to peripheral nerve regeneration in the aging nervous system and may provide therapeutic targets to enhance repair and treat age-associated neuropathies.

MATERIALS AND METHODS

Animals and Surgery

1. Differential Gene Expression

23 mice of the C57BL/6J strain were obtained from Jackson Laboratories. Of these mice, 11 were classified as "young" with a mean age of 8.3 weeks at the time of injury (standard deviation = 1.9 weeks, range = 5.1 weeks). 12 were classified as "old" with a mean age of 73.1 weeks at the time of injury (standard deviation = 6.3 weeks, range = 18.0 weeks). Peripheral nerve injuries were performed as previously described (Tomlinson, Žygelytė, Grenier, Edwards, & Cheetham, 2018). All 23 mice in the study were induced at 5% isoflurane and maintained at 1.5-3.5% isoflurane. Mice were administered a pre-operative dose of Saline (0.3 mL) and Firocoxib (0.02 mL) subcutaneously, as well as an additional dosage of 0.02 mL Firocoxib (20 mg/mL) subcutaneously 24 hours after surgery.

A skin incision was made in the left mid-thigh, the biceps was dissected, and the sciatic nerve exposed. The nerve was transected proximal to the bifurcation. The proximal and distal stumps of the nerve were then aligned and sutured into a 5mm conduit [1.98mm ID] using a 10-0 Ethilon.

2. Assessing Motor Function Recovery

11 mice of the C57BL/6J strain were obtained from Jackson Laboratories. Of these mice, 5 were classified as "young" with a mean age of 12 weeks at the time of injury. 6 were classified as "old" with a mean age of 108 weeks at the time of injury.

I also performed a preliminary study to test peripheral nerve regeneration in a mammal with regenerative capacities, the African Spiny mouse (*Acomys Cahirinus*). This animal was obtained from a breeding colony at Cornell University. All 12 mice were anesthetized and

maintained at 3% isoflurane. The hair on the entire left flank, leg, and lower half of the back was removed with a razor and Nair. The mice were administered a dose of Saline (0.3 mL) and Buprenorphine (0.05 mL) subcutaneously. They were then tattooed at the left stifle, hock, distal metatarsal, and rib point using a No. 5R needle tube, No. 1005RL needle, and "BLACK ONYX Millennium Mom's Tattoo Ink".

In a different procedure, all 12 mice in the study were induced at 5% isoflurane maintained at 1.5-2.5% isoflurane. Mice were administered a pre-operative dose of Saline (0.3 mL) and Buprenorphine (0.0515 mL) subcutaneously, as well as an additional dosage of 0.05 mL Buprenorphine (0.0515 mg/mL) subcutaneously 24 hours after surgery.

A skin incision was made in the left mid-thigh, the biceps was dissected, and the sciatic nerve exposed. The tibial branch of the sciatic nerve was separated and transected distal to the nerve's attachment point to the femoris muscle. A 10-0 Ethilon suture was used to repair the tibial transection through direct anastomosis.

No sham surgeries were done. All studies were performed in accordance with the PHS Policy on Humane Care and Use of Laboratory Animals, the NIH guide for Care and Use of Laboratory Animals, federal and state regulations, and was approved by the Cornell University Institutional Animal Care and Use Committee (IACUC, protocol #2012-0099). Animals were brought into the research unit and given a 5 day acclimatization period prior to any procedure. All animals were maintained in a temperature and light controlled environment (12 hour light/dark cycle) and were permitted *ad libitum* access to water and standard laboratory rodent food (Tekland Mouse Breeder Diet, Harlan Laboratories, Madison, WI) without restriction. ARRIVE guidelines for reporting *in vivo* experiments were used throughout.

Macrophage Isolation from Regenerative Bridges and RNA Extraction

Macrophage isolation from regenerative bridges and RNA extraction was performed as previously described (Tomlinson et al., 2018). Mice were euthanized 5 days after repair and the regenerative bridge was harvested within the conduit by transecting the proximal and distal sciatic nerve stumps ~1.0mm from the ends of the conduit. The regenerative bridge was placed in a petri dish with 1mL of digestion media, the sutures and conduit were removed, then the nerve was cut into 1-2mm pieces. The pieces were then transferred to a 50mL conical with digestion media and incubated for 1 hour at 37°C in a hot water bath. After incubation, the media was strained through a 70-μm nylon filter (BD Biosciences) to obtain a single-cell suspension. Cells were centrifuged at 300 g for 10 minutes and resuspended in 200μL 0.5%BSA in PBS. Macrophages were isolated based on surface markers via flow cytometry, following the method outlined in Tomlinson et al., 2018. For this method, cells were plated on a v-bottom 96 well plate for FACS and labeled for 45 minutes at 4°C using species-specific antibodies to label macrophages and other immune cells. Antibody details are provided in Table 1. Non-macrophage cell markers were used to confirm the specificity of the sort. All wash steps were done with 0.5%BSA in PBS. After sorting, cells were placed into RNase/DNase-free 1.5-mL tubes and RNA was purified according to manufacturer's instructions using the Quick-RNA MicroPrep kit (Zymo Research).

Table 1. Antibodies used for flow cytometric sorting of macrophages from injured sciatic nerve.

Antibodies	**Ab source**	**Ab Lot#**	**Target**	**Clone**	**Conjugate**	**Ab storage**
Thy1.2	eBioscience 17-0902-81	E07186-1635	Fibroblast	53-2.1	APC	4*C
Ter119	eBioscience 17-5921-82	E07331-1635	RBC	Ter119	APC	4*C
Ly6G	eBioscience 17-9668-82	E20219-105	Granulocyte	1A8-Ly6g	APC	4*C
CD19	eBioscience 17-0193-82	E10736-1634	B cell	eBio ID3	APC	4*C
CD3e	eBioscience	E12535-109	T cell	17A2	APC	4*C

	17-0032-82					
CD14	eBioscience 12-0141-82	E01090-1632	Macrophage	Sa2-8	PE	4*C
CD31	BD 551262	4129872	Endothelial cell	MEC 13.3	APC	4*C
CD16/32	BD 563006	5260724	Macrophage (not specific)	2.4G2	BV605	4*C
F4/80	eBioscience 25-4801-82	E07631-1637	Macrophage	BM8	PE-Cy7	4*C
SiglecF (SF-M)	Miltenyi 130-102-241	5150727311	eosinophil		APC	4*C
UltraComp eBeads	eBioscience 01-2222-42	4296349	For compensation			4*C
CD11b	BioLegend 101224	B196387	Macrophage (not specific)	M1/70	Pacific Blue	4*C
PI	eBioscience 00-6990-50	E00030-1638	Dead cell/DNA			4*C

RNA Sequencing

RNA sequencing was performed off-site, according to the protocol described by Tomlinson et al., 2018. Spectrophotometry was used to confirm RNA sample quality and determine concentration and chemical purity (A260/230 and A260/280 ratios), and a Fragment Analyzer was used to determine RNA integrity. The NEBNext Poly(A) mRNA Magnetic Isolation Module isolated PolyA+RNA, and TruSeq-barcoded RNA Sequencing (RNASeq) libraries were generated with the NEBNext Ultra RNA Library Prep Kit. Libraries were quantified with a Qubit 2.0, with size distribution determined with a Fragment Analyzer. The libraries were then sequenced on an Illumina NextSeq500 and reads trimmed for low quality and adaptor sequences. Tophat v2.0 was used to map reads to the reference genome (Mouse: UCSC mm10).

Gene Expression Analysis with NanoString

To highlight genes important to the study, extracted RNA was incubated with a panel of probes specific for genes involved with macrophage phenotype and function. Following standard NanoString protocol, reporter probes, hybridization solution, sample, and capture probes were

mixed and hybridize at 65°C overnight. Processing of the samples in the NanoString nCounter Prep Station purified the target/probe complexed which were then immobilized in a cartridge for data collection. NanoString nSolver 2.6 Analysis Software was used to process raw data, and genes with average expression in all groups below background expression were removed from analysis (Tomlinson et al., 2018).

Hierarchical Clustering and Statistical Analysis

Average linkage hierarchical clustering was performed using Heatmapper.ca according to log2-fold change values. The Heatmapper.ca software was used to find the average of all expression values across the sample size for a given gene, and the expression value of for each sample was subsequently divided by the average gene expression across the group to determine whether the gene is over- or under-expressed. In average linkage clustering, the distance between each pair of observations within a cluster was summed and divided by the number of pairs, giving an average cluster distance. A dendrogram was created by grouping clusters that have the most similar average cluster distance together. Analyzing clustering and dendrograms in heatmaps can provide insight on which genes have similar trends in their differential expression between the old and young conditions.

Following mapping, Cufflinks v2.2 generated FPKM values and statistical analysis of differential gene expression. Cuffdiff output provides the results of the statistical test for differential expression with an output of “yes” or “no” depending on if the p-value and q-value, adjusting for the false discovery rate, are less than 0.05. Further stringent cutoffs for differential gene expression of a fold-change value greater than 2 and a FPKM value greater than 2 for at least

one of the conditions were applied to the data. A gene must meet all three of these criteria in order to qualify as a stringent differentially expressed gene.

Differential gene expression data was also analyzed using Downstream Effects Analysis in Ingenuity Pathway Analysis (IPA), a web-based software application that groups genes based on biological functions that are expected to increase or decrease according to gene expression changes. The changes in expression levels of genes in the dataset were compared to literature in the software's knowledge base and a p-value was calculated using a Right-Tailed Fisher's Exact Test. This p-value served as an indication of how likely the overlap between a set of significant genes from the experiment and a given biological pathway was random. The smaller the p-value, the less likely the association was random, meaning that the significant genes were more likely to impact the functionality of the associated biological pathway.

Walking Track Design

The walking track apparatus consisted of a ~1 meter Plexiglass chamber with a mirror placed at an angle 45° to the bottom panel. The distance between the start and end markers was 30 cm. A Basler ACA1920-155uc 1920x1200 camera running at 120 frames per second with an attached Fujicon model CF25HA-1 25mm focal length lens was set up on a tripod to have a direct view of the front of the track. Prior to surgery, all mice were subjected to a three-day acclimation period in which they ran down the track with the encouragement of an air gun until they ran at an even pace with no jumping motions. Each run was repeated 5-8 times per mouse on all three days. Once the animals were acclimated to the track, two days of baseline videos were taken of 5 runs per mouse on each day before the surgery was done. This same procedure was repeated for each mouse each week for 15 weeks post-operation.

Gait Analysis

The video was recorded using Basler Pylon software and encoded into MJPEG format using Pixvideo MJPEG codec ver 4.017. Gait tracking of the marker points was done using SIMI Motion ver 9.2.2 software package and analyzed using custom scripts developed in Mathworks Matlab. Marker points included the stifle, hock, and metatarsal head to find the hock angle during mid-stance on the injured side.

Peak Tetanic Force

After 15 weeks of gait tracking, the peak tetanic force of the mouse gastrocnemius muscle was taken using an Aurora Scientific Dual Mode Lever System, Master 8 box voltage stimulator, and AD Instruments Power Lab to collect data. The mice were induced with 5% isoflurane, maintained at 1.5-2% isoflurane. An incision was made in the mid-thigh of the injured side and the gastrocnemius muscle and sciatic nerve were exposed. The common peroneal and sural branches of the sciatic nerve were transected, keeping the tibial branch intact. The distal tendon to the gastrocnemius muscle was secured with a silk 6-0 suture proximal to the calcaneus to help align it to the lever arm, and the limb immobilized on a metal platform. Two electrodes connected to the pulse stimulator were placed on the tibial nerve. Once the voltage and length of the muscle were optimized, the muscle was stimulated with a biphasic wave of duration 200μs for each phase and a 50μs delay between cathodic and anodic phases at 100 Hz frequency. This was repeated three times with a 7-minute interval between each measurement. The same process was repeated on the uninjured side. By comparing the muscle peak tetanic force output on the injured side to the uninjured side, conclusions can be made on the degree of motor function recovery, thus

reinnervation, in the animal. Due to the relationship between nerve injury and muscle atrophy, the muscle innervated by the nerve in study can be harvested, and the ratio of its weight on the injured side to the uninjured side can also serve as an indication of reinnervation.

Muscle Harvests

After the determination of peak tetanic force, the mouse was euthanized with 1.0mL of Fatal Plus. The gastrocnemius muscle was separated by cutting the proximal and distal attachments, and the muscle weight recorded. This was performed for both the injured and the uninjured site. As muscle atrophy is a natural consequence of aging, the ratio of uninjured to injured side within the same animal can serve to control for any changes in muscle mass that may occur with age.

RESULTS

Differential Gene Expression

In order to determine differences in macrophage phenotype and function following injury, RNA sequencing was performed on macrophages isolated from regenerative bridges following sciatic nerve injury. Gene expression was then quantified using RNASeq and compared between old and young mice. Of 23,360 identified genes, 14,044 were tested for differential gene expression as expression levels in the other genes were too low to test. Of the genes tested, 90 genes met the stringent-DE cutoff of having a p-value and q-value < 0.05, a fold-change value > 2, and a FPKM > 2 for at least 1 condition. Hierarchal clustering revealed two clusters of genes that had markedly different expression levels in young and old mice after peripheral nerve injury (Figure 1). The genes of cluster 1 were upregulated in young mice in comparison to old mice.

Some of these genes included *Agtr2*, *Ifit1*, *Ifit3*, *Gap43*, *Dlk1*, *Mx2*, *Ugt8a*, and *Fa2h*. The genes of cluster 2 were upregulated in old mice in comparison to young mice. Some of these genes included *Lep*, *Il11*, *Adam8*, *Mmp12*, *Gjb1*, and *Il17b*.

Differentially expressed genes were then analyzed to identify which biological processes and functions were affected by their up- and downregulation using Downstream Effects Analysis through IPA. IPA identified STAT3, dexamethasone, TNF, Lipopolysaccharide, and IFNγ as top upstream regulators that affect macrophage polarization (Figure 2A). The key pathways affected by differential gene expression are axonal guidance signaling, immune function (agranulocyte adhesion and diapedesis, granulocyte adhesion and diapedesis), the osteoarthritis pathway, and atherosclerosis signaling (Figure 2B). The p-value output from IPA provides insight in how random the overlap between the genes in the data set and the pathways they affect are. The smaller the p-value, the less random the association between the genes and the pathways is.

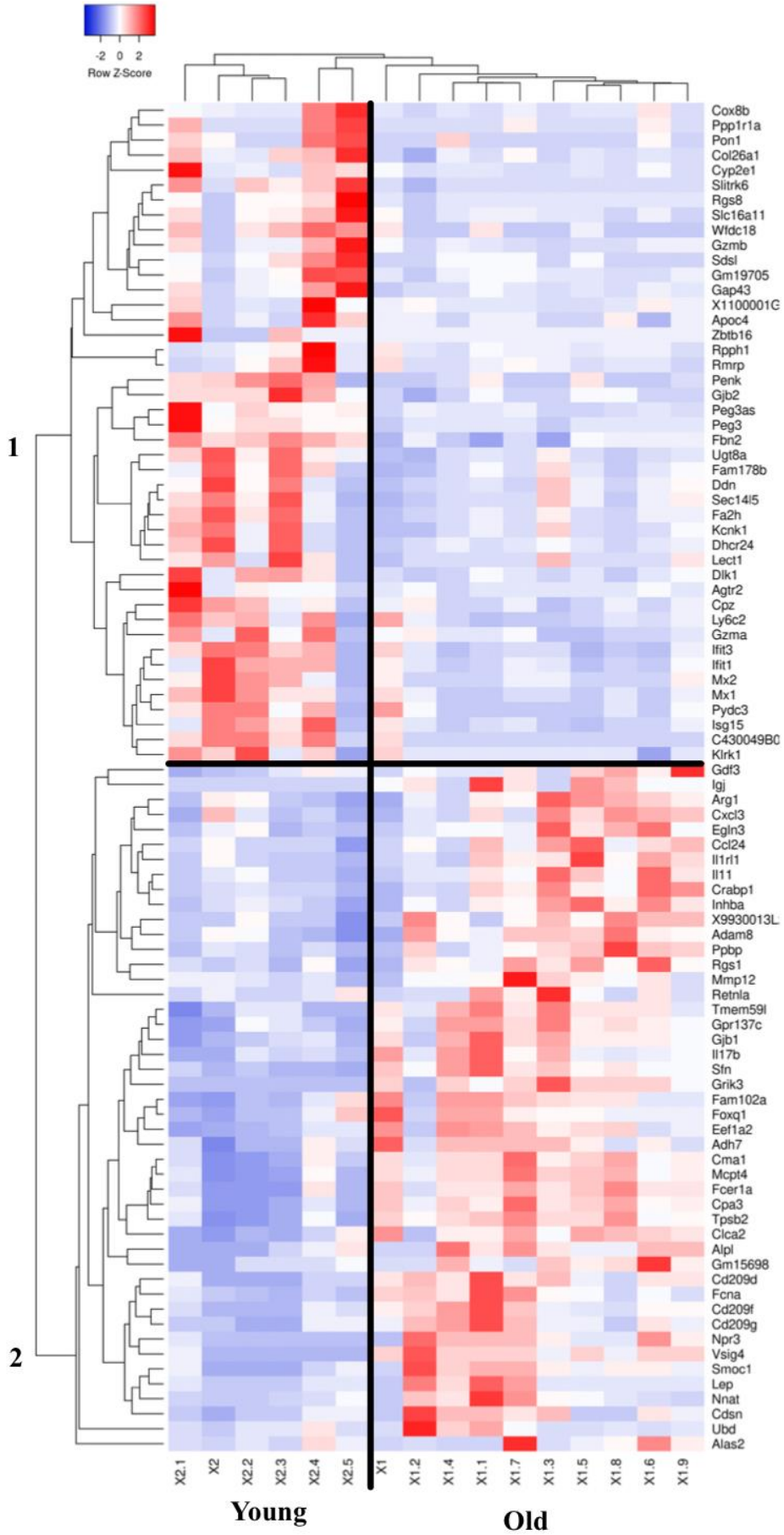
-2 0 2
Row Z-Score
Cox8b
Ppp1r1a
Pon1
Col26a1
Cyp2e1
Slitrk6
Rgs8
Slc16a11
Wfdc18
Gzmb
Sdsl
Gm19705
Gap43
X1100001G
Apoc4
Zbtb16
Rpph1
Rmrp
Penk
Gjb2
Peg3as
Peg3
Fbn2
Ugt8a
Fam178b
Ddn
Sec14l5
Fa2h
Kcnk1
Dhcr24
Lect1
Dlk1
Agtr2
Cpz
Ly6c2
Gzma
Ifit3
Ifit1
Mx2
Mx1
Pydc3
Isg15
C430049B0
Klrk1
Gdf3
Igj
Arg1
Cxcl3
Egln3
Ccl24
Il1rl1
Il11
Crabp1
Inhba
X9930013L
Adam8
Ppbp
Rgs1
Mmp12
Retnla
Tmem59l
Gpr137c
Gjb1
Il17b
Sfn
Grik3
Fam102a
Foxq1
Eef1a2
Adh7
Cma1
Mcpt4
Fcer1a
Cpa3
Tpsb2
Clca2
Alpl
Gm15698
Cd209d
Fcna
Cd209f
Cd209g
Npr3
Vsig4
Smoc1
Lep
Nnat
Cdsn
Ubd
Alas2
1
2
X2.1
X2
X2.2
X2.3
X2.4
X2.5
X1
X1.2
X1.4
X1.1
X1.7
X1.3
X1.5
X1.8
X1.6
X1.9
Young
Old

Figure 1. Hierarchical clustering on differential gene expression between young (X2-X2.5, n=6, age=~6 weeks) and old (X1-X1.9, n=10, age=~73 weeks) mice revealed 2 clusters of differentially expressed genes after peripheral nerve injury. The genes of cluster 1 are upregulated in young mice and downregulated in old mice, meaning that these genes are expressed at a higher level in younger mice compared to expression levels in old mice. The genes of cluster 2 are upregulated in old mice and downregulated in young mice, meaning that these genes are expressed at a higher level in older mice compared to expression levels in young mice. Gene expression was compared between two age groups and 90 genes met the stringent differential expression parameters. Hierarchical clustering between the two experimental conditions of young and old confirmed transcriptional similarities between animals of the same age classification.

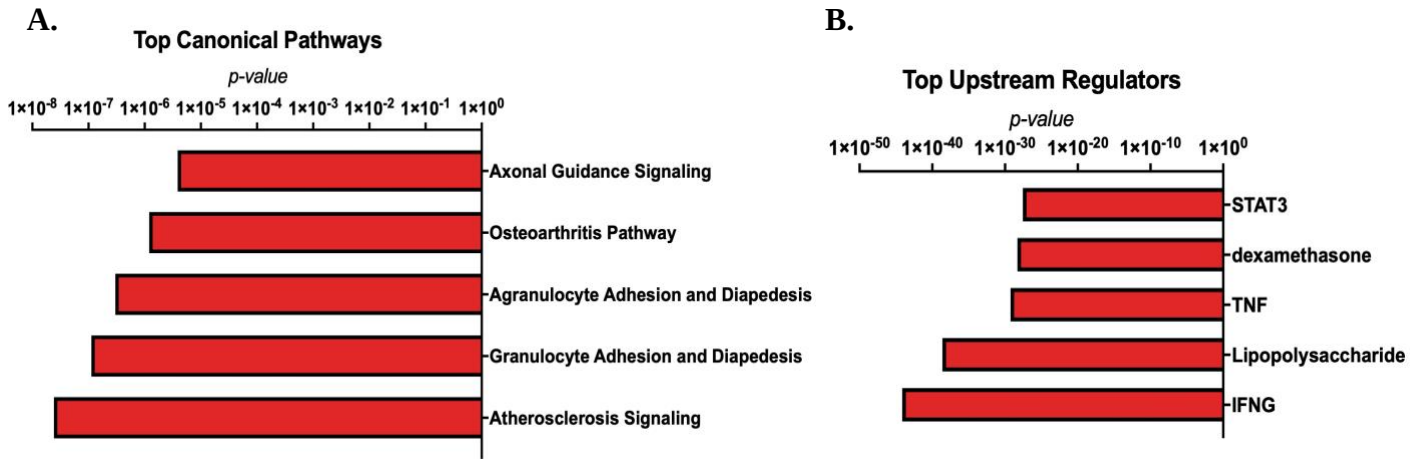

Figure 2. A. Key pathways identified by IPA to be affected by the differential gene expression between young and old mice. P-values indicate the degree to which the association between the differential expressed genes and the pathways is random. **B.** Key upstream regulators identified by IPA to be affected by the differential gene expression between young and old mice. P-values indicate the degree to which the association between the differential expressed genes and the pathways is random.

Assessing Motor Function Recovery

1. Gait analyses

In order to understand differences in how young, old, and spiny mice reinnervate muscle and recover motor function after peripheral nerve injury, gait analyses were performed weekly for 15 weeks after tibial nerve transection and anastomosis. As seen in Figure 3, motor function in all animals in all three groups was impaired at week 2 as seen by a ~50% reduction in hock angle

after peripheral nerve injury. There was some recovery of hock angle by week 12 for young and old mice, however, hock angles for these two groups decreased again to around 50% in week 15. After week 12, the spiny mouse continued to recover to around 75% of the baseline hock angle by week 15. Despite the deviation in hock angles between the C57 mice and the spiny mice after week 12, none of the differences are statistically significant.

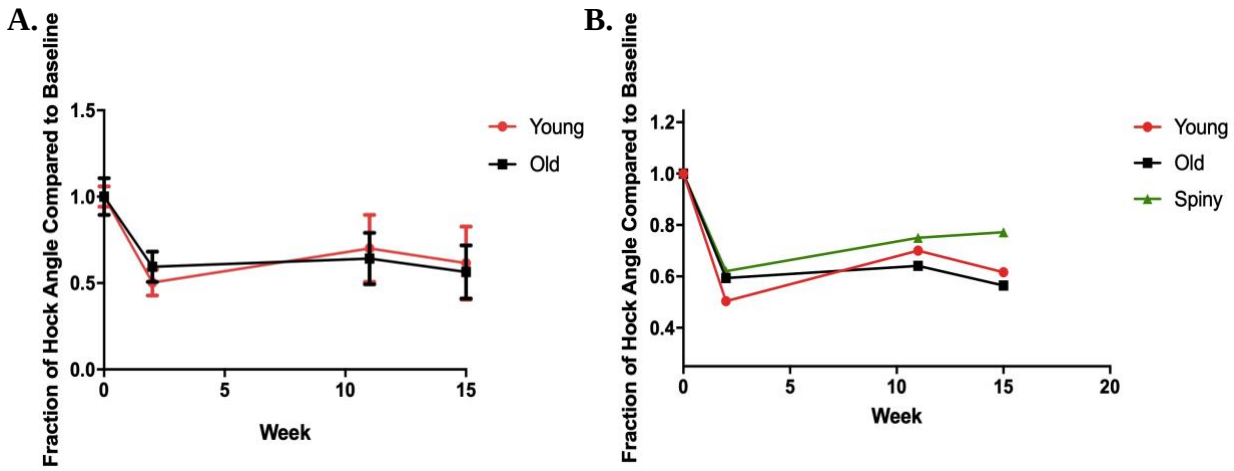

Figure 3. A. Gait tracking of hock angles after peripheral nerve injury in young (n=5, age=~12 weeks) and old (n=6, age=~108 weeks) C57 mice. **B.** Gait tracking of hock angles after peripheral nerve injury in young and old C57 mice compared to the African spiny mouse, *Acomys Cahirinus* (n=1). The spiny mouse only drops to 60% functionality after tibial nerve transection and repair and recovers to around 80%. However, the difference between recovery in the C57 mice and the spiny mouse is not statistically significant. This figure was made from work done in conjunction with William Miklavcic.

2. Muscle force measurements

In order to further assess functional recovery after peripheral nerve injury, the peak tetanic force of the gastrocnemius muscle was measured to investigate strength of contraction, and the muscle harvested 15 weeks post-operation. The ratios of the gastrocnemius muscle weights on the injured and uninjured side were close to one (Figure 4A). While the ratio was slightly larger for older mice than younger mice, the difference between the two groups was not statistically

significant. The gastrocnemius muscle weights on both sides were also compared to the animal's body weight to account for the positive correlation between body size and muscle size (Figure 4B, 4C). In this comparison, the gastrocnemius muscle was smaller compared to body weight in old mice on both the injured left side and the uninjured right side, however, this difference was not statistically significant from the ratio in younger mice. Peak tetanic force measurements provide an indication of muscle reinnervation. The ratios of the peak tetanic force measured on the left to right side were calculated and compared between young and old mice (Figure 4D). Younger mice were found to have slightly larger peak tetanic force measurements on their injured side than older mice, but this difference was not statistically significant. The ratios of the peak tetanic force relative to muscle weight on the left to right side were calculated and compared to adjust for the direct relationship between muscle weight and peak tetanic force Figure 4E). Younger mice were revealed to have twice as strong peak tetanic force on their injured side compared to their uninjured side while the relationship was near even on both sides for older mice. The differences between the two groups were not statistically significant.

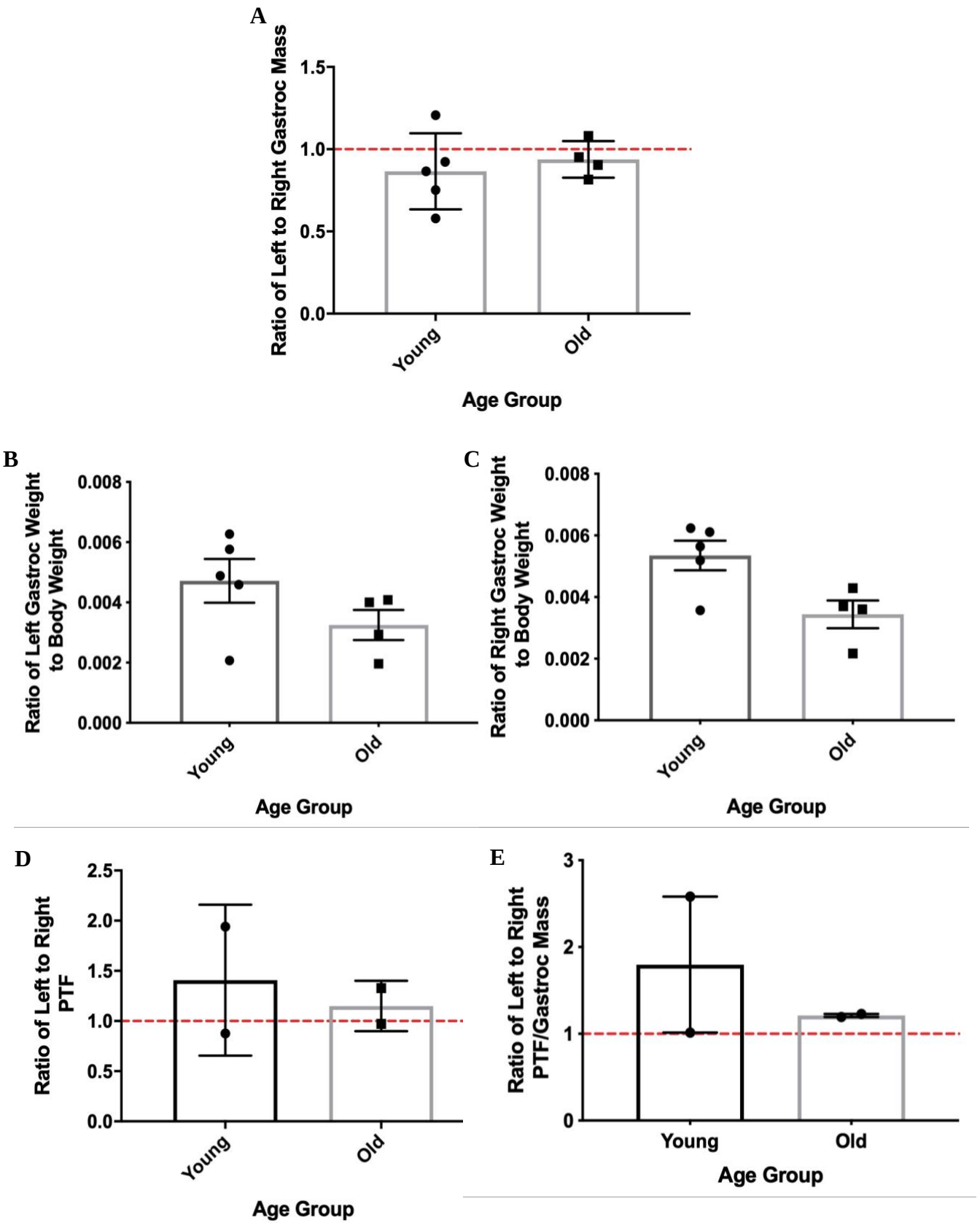
A
Ratio of Left to Right Gastroc Mass
1.5
1.0
0.5
0.0
Young
Old
Age Group
B
Ratio of Left Gastroc Weight to Body Weight
0.008
0.006
0.004
0.002
0.000
Young
Old
Age Group
C
Ratio of Right Gastroc Weight to Body Weight
0.008
0.006
0.004
0.002
0.000
Young
Old
Age Group
D
Ratio of Left to Right PTF
2.5
2.0
1.5
1.0
0.5
0.0
Young
Old
Age Group
E
Ratio of Left to Right PTF/Gastroc Mass
3
2
1
0
Young
Old
Age Group

Figure 4. A. The ratio of left to right gastrocnemius muscle weights was compared between young (n=5, age=~12 weeks) and old (n=4, age=~108 weeks) mice. There were no significant differences between the ratio of muscle weights between young and old mice. **B.** In comparing the weight of the gastrocnemius muscle from the injured left side to the animal's body weight, no significant differences were found. **C.** In comparing the weight of the gastrocnemius muscle from the uninjured right side to the animal's body weight, no significant differences were found. **D.** Comparison of the ratios of the peak tetanic force produced by the gastrocnemius muscle on the left to right side between young and old animals revealed no significant differences. **E.** Comparison of the ratios of the peak tetanic force produced by the gastrocnemius muscle relative to the muscle weight on the left to right side between young and old animals revealed no significant differences. This figure was made from work done in conjunction with William Miklavcic.

DISCUSSION

In studying the differential gene expression of macrophages between young and old mice after peripheral nerve injury, it was revealed that many of the major immune and inflammatory pathways and regulators involved in the peripheral nerve recovery pathway were affected by aging. Hierarchical clustering of the 90 stringent differentially expressed genes divided genes into two clusters that are differentially regulated in young and old mice.

The genes of cluster 1 were upregulated in young mice in comparison to old mice. Some of these genes are involved in the immune response triggered after nerve injury, such as *Agtr2*, *Ifit1*, and *Ifit3*, and are known to be expressed in macrophages that infiltrate the injury site (Lisi et al., 2017; Shepherd et al., 2018). Other up-regulated genes in young mice included *Gap43*, *Dlk1*, and *Mx2*, which promote cell proliferation and neurogenesis (Kunz et al., 2009; Surmacz et al., 2012; Williams, Venkatesh, Pearse, Udvadia, & Bunge, 2015). Additionally, expression of *Ugt8a* and *Fa2h*, genes that encode enzymes in the biosynthesis pathway for myelin membrane, are over-expressed in young animals (Furukawa, Ohmi, Ohkawa, Tajima, & Furukawa, 2014; Olsen & Færgeman, 2017). The upregulation of these genes in young mice suggests that the initiation of

peripheral nerve regeneration by these genes occurs at higher levels in young animals than in old animals.

The genes of cluster 2 were upregulated in old mice in comparison to young mice. One of these genes, *Lep*, produces leptin, a molecule known to stimulate macrophages after peripheral nerve injury (Maeda et al., 2009). Other genes of interest in this cluster included *Il11*, *Adam8*, *Mmp12*, and *Gjb1*, which are involved in nerve regeneration by de-differentiating and proliferating Schwann cells and by myelinating new axons (Barrette et al., 2008; Cheng, Wang, Yu, & Yi, 2017; Kleopa, Abrams, & Scherer, 2012; H. Liu et al., 2010). The upregulation of these genes in old mice suggests that the initiation of peripheral nerve regeneration by these genes occurs at higher levels in old animals than in young animals. This is contrary to the hypothesis that old animals may have a reduced capacity for peripheral nerve regeneration due to transcriptional differences. Another highly expressed gene in old mice was *Il17b*—over-expression of this group of interleukins is known to have an inhibitory effect on neural stem cell proliferation and differentiation (Li et al., 2013). While other differentially expressed genes between old and young animals activate similar downstream peripheral nerve regeneration pathways such as axonal guidance and immune functions, the over-expression of *Il17b* in old mice may explain some observed impairment in their ability to recover after peripheral nerve injury.

Analysis of these data with IPA indicated which pathways and biological functions are most affected by age and their role in peripheral nerve regeneration. IPA uses data to produce a p-value indicating the degree of how random the association between the genes of the data set and the affected biological pathways is random. The smaller the p-value, the less random the association, meaning that the significant genes are more likely to be correlated with that biological pathway. One of the pathways affected, axonal guidance signaling had a p-value of $3.87*10^{-6}$ (Figure 2A)

and is directly involved in nerve regeneration by properly guiding axons to their targets to form synaptic connections (Russell & Bashaw, 2018). The results of this study suggest that aging alters gene expression to affect the guidance of axons during regeneration after nerve injury. This may partially explain the delay in peripheral nerve regeneration in older animals.

Other major pathways studied in this experiment included agranulocyte and granulocyte adhesion and diapedesis (Figure 2A). As noted in previous studies, these pathways exhibit sustained activation during peripheral nerve regeneration and indicate an involvement of the immune and inflammatory system in nerve regeneration (Xing, Cheng, Zha, & Yi, 2017). In this study, they were noted to have a non-random association with differential gene expression between young and old mice after peripheral nerve injury. This suggests that aging causes a transcriptional alteration that affects the expression of this pathway, thus correlating with any differences seen in the ability of old and young mice to regenerate after peripheral nerve injury.

All of the upstream regulators found through IPA to have significant association with the differential gene expression between young and old mice after peripheral nerve injury were involved in the inflammatory and immune system (Figure 2B). STAT3 specifically is involved in cell growth, proliferation, and movement (Benito et al., 2017). Much of the regenerative process after peripheral nerve regeneration includes these processes as neurons grow and Schwann cells and macrophages are recruited to the area to clear debris (Painter et al., 2014). Other regulators seen to have an association with the differential gene expression data are dexamethasone, TNF, Lipopolysaccharide, and IFNγ, all of which are involved in enhancing phagocytosis and increasing pro-inflammatory responses. Because all of these regulators were affected by differential gene expression between young and old mice after peripheral nerve injury, age may have an effect in

how these regulators regulate certain pathways that allow peripheral nerves to regenerate. This could then explain why older animals have a reduced regenerative capacity.

For this study, RNA expression was studied post-injury specifically, since I am interested in examining age-related differences in peripheral nerve regeneration in the post-injury environment. I was able to identify clear differences between the age groups; however, I was not able to include studies on RNA-expression in non-injured animals within the current series. While this limits my interpretation of the results, since some changes may not represent true injury-related changes, the study does give the clinical picture of what happens following peripheral nerve injury.

Assessing motor function also serves as an additional parameter in understanding how peripheral nerve recovery and muscle reinnervation may differ between young and old animals. As seen in previous studies, gait analysis of hock angle and measurement of peak tetanic force are both valid parameters to asses motor function recovery (Lee et al., 2013). Gait analysis of the hock angle in both young and old mice revealed very little recovery in motor function in both age groups (Figure 3A). Hock angle measurements in the spiny mouse (Figure 3B), however, revealed slightly more recovery in this species, possibly due to *Acomys*'s superior regenerative properties (Seifert et al., 2012).

Despite my preliminary data implying age-related differences in neuromuscular function, gait analyses may be less sensitive in this quadruped animal model than in humans to reveal subtle age-related differences following peripheral nerve injury. This may be due to compensatory changes, such as offloading weight from the injured limb on to the contralateral hindlimb and forelimbs. In addition, since sensory function recover more quickly than motor activity, sensory proprioceptive feedback may engage contralateral musculature to maintain appropriate position (or "hip-hike") observed in many species following limb injury, and similar mechanisms may permit sensory

proprioceptive feedback via the femoral nerve to compensate adjust limb position during lack of sciatic motor circuit feedback (Zigmond & Echevarria, 2019).

Peak tetanic force measurements and gastrocnemius muscle weights specifically explored muscle reinnervation after tibial nerve injury. Muscle mass ratios between the injured and uninjured side were close to 1 for both young and old mice (Figure 4A), indicating that enough reinnervation of the left gastrocnemius muscle occurred to counter any muscle atrophy caused by nerve injury in both age groups. However, when comparing the weight of the muscle to body weight of each side individually, both the left and right sides showed that the gastrocnemius muscle was a smaller proportion of body weight in old animals than in young animals (Figure 4B, 4C). As this difference between the two age groups was seen on both the uninjured and the injured side, it may be accountable to natural muscle atrophy with age rather to nerve injury and reduced recovery.

Ratios of peak tetanic force measurements on the left side to the right side showed that the ratio was higher in young mice than in old mice (Figure 4D, 4E). This means that force output for the injured left side was greater than the force output for the uninjured right side in younger mice. While previous studies have shown a range from some to full motor function recovery after peripheral nerve regeneration (Ma et al., 2011; Painter et al., 2014), there has been little observation of post-nerve injury motor function exceeding function prior to any injury. The peak tetanic force data also does not match the gastrocnemius muscle weights or gait analysis data. As reinnervation does not necessarily mean that the nerves regrew the same way the originally were, reinnervation could have created new neuromuscular junctions that allowed the muscle to create a substantial force measurement but did not restore regular gait. It is also possible that a smaller sample size for both age groups for the peak tetanic force measurements precluded us from being

able to observe differences between experimental groups. However, further analyses will be needed to clarify.

Previous studies have discovered that old animals can regain full recovery after peripheral nerve injury, but the process of this recovery is delayed in older mice (Painter et al., 2014). It is possible that, if more points were analyzed between weeks 2 and 12 in the gait experiment (Figure 3), old mice would have had a slower recovery rate than young mice. Future studies that could be done are comparing the temporal differences in peripheral nerve recovery between young and old mice. Analyses may be performed at various time points after injury to better assess the temporal differences between functional recovery in young and old animals.

While I did not observe impaired recovery of motor function in old animals when I compared them to young animals, this study did identify many inflammatory and immune system responses that are involved in peripheral nerve regeneration and differ in their expression between young and old mice. This study is important because it identifies a number of pathways through which macrophages may influence peripheral nerve regeneration in different age groups. These pathways may be important in providing therapeutic targets to treat age-associated neuropathies.

ACKNOWLEDGMENTS

I thank Dr. Jonathan Cheetham for allowing me the opportunity to conduct this research and for all of the advice, knowledge, and academic and professional support he has given me during my time at Cornell University, Michael Sledziona for help in carrying out the methods required for this experiment, and Dr. Fiona Inglis for critical comments on the manuscript. I also thank Alicia Brunson for help in carrying out the differential gene expression experiment and William Miklavcic for help in carrying out the functional recovery experiment. Finally, I would

like to thank my advisors at Cornell University's Office of Undergraduate Biology, specifically Dr. Laura Schoenle and Dr. Mark Roberson. This work was supported by a RO1 Award to Jonathan Cheetham from the National Institute of Deafness and Communication Disorders.

REFERENCES

Araki, T., Nagarajan, R., & Milbrandt, J. (2001). Identification of Genes Induced in Peripheral Nerve after Injury. *The Journal of Biological Chemistry*, *276*(36), 34131–34141. https://doi.org/10.1074/jbc.M104271200

Barrette, B., Hebert, M.-A., Filali, M., Lafortune, K., Vallieres, N., Gowing, G., … Lacroix, S. (2008). Requirement of Myeloid Cells for Axon Regeneration. *Journal of Neuroscience*, *28*(38), 9363–9376. https://doi.org/10.1523/JNEUROSCI.1447-08.2008

Benito, C., Davis, C. M., Gomez-Sanchez, J. A., Turmaine, M., Meijer, D., Poli, V., … Jessen, K. R. (2017). STAT3 controls the long-term survival and phenotype of repair schwann cells during nerve regeneration. *The Journal of Neuroscience*, *37*(16), 4255–4269. https://doi.org/10.1523/JNEUROSCI.3481-16.2017

Cattin, A.-L., Burden, J. J., Van Emmenis, L., Mackenzie, F. E., Hoving, J. J. A., Garcia Calavia, N., … Lloyd, A. C. (2015). Macrophage-Induced Blood Vessels Guide Schwann Cell-Mediated Regeneration of Peripheral Nerves. *Cell*, *162*(5), 1127–1139. https://doi.org/10.1016/j.cell.2015.07.021

Cattin, A. L., & Lloyd, A. C. (2016, August 1). The multicellular complexity of peripheral nerve regeneration. *Current Opinion in Neurobiology*. Elsevier Ltd. https://doi.org/10.1016/j.conb.2016.04.005

Chen, Z.-L., Yu, W.-M., & Strickland, S. (2007). Peripheral Regeneration. *Annual Review of Neuroscience*, *30*(1), 209–233. https://doi.org/10.1146/annurev.neuro.30.051606.094337

Cheng, Q., Wang, Y. X., Yu, J., & Yi, S. (2017). Critical signaling pathways during Wallerian degeneration of peripheral nerve. *Neural Regeneration Research*, *12*(6), 995–1002. https://doi.org/10.4103/1673-5374.208596

Cho, D. Y., Mold, J. W., & Roberts, M. (2006). Further investigation of the negative association between hypertension and peripheral neuropathy in the elderly: An Oklahoma Physicians Resource/Research Network (OKPRN) study. *Journal of the American Board of Family Medicine*, *19*(3), 240–250. https://doi.org/10.3122/jabfm.19.3.240

Fu, S. Y., & Gordon, T. (1997). The cellular and molecular basis of peripheral nerve regeneration. *Molecular Neurobiology*, *14*(1–2), 67–116. https://doi.org/10.1007/BF02740621

Furukawa, K., Ohmi, Y., Ohkawa, Y., Tajima, O., & Furukawa, K. (2014). Glycosphingolipids in the regulation of the nervous system. *Advances in Neurology*, *9*, 307–320. https://doi.org/10.1007/978-1-4939-1154-7_14

Gaudet, A. D., Popovich, P. G., & Ramer, M. S. (2011, August 30). Wallerian degeneration: Gaining perspective on inflammatory events after peripheral nerve injury. *Journal of Neuroinflammation*. BioMed Central. https://doi.org/10.1186/1742-2094-8-110

Gomez-Sanchez, J. A., Carty, L., Iruarrizaga-Lejarreta, M., Palomo-Irigoyen, M., Varela-Rey, M., Griffith, M., … Jessen, K. R. (2015). Schwann cell autophagy, myelinophagy, initiates myelin clearance from injured nerves. *Journal of Cell Biology*, *210*(1), 153–168. https://doi.org/10.1083/jcb.201503019

Huebner, E. A., & Strittmatter, S. M. (2009). Axon regeneration in the peripheral and central nervous systems. *Results and Problems in Cell Differentiation*, *48*, 339–351. https://doi.org/10.1007/400_2009_19

Kleopa, K. A., Abrams, C. K., & Scherer, S. S. (2012, December 3). How do mutations in GJB1 cause X-linked Charcot-Marie-Tooth disease? *Brain Research*. NIH Public Access. https://doi.org/10.1016/j.brainres.2012.03.068

Kunz, D., Walker, G., Bedoucha, M., Certa, U., März-Weiss, P., Dimitriades-Schmutz, B., & Otten, U. (2009). Expression profiling and Ingenuity biological function analyses of interleukin-6-versus nerve growth factor-stimulated PC12 cells. *BMC Genomics*, *10*(90). https://doi.org/10.1186/1471-2164-10-90

Lee, J.-Y., Giusti, G., Wang, H., Friedrich, P. F., Bishop, A. T., & Shin, A. Y. (2013). Functional evaluation in the rat sciatic nerve defect model: a comparison of the sciatic functional index, ankle angles, and isometric tetanic force. *Plastic and Reconstructive Surgery*, *132*(5), 1173–1180. https://doi.org/10.1097/PRS.0b013e3182a3bfeb

Li, Z., Li, K., Zhu, L., Kan, Q., Yan, Y., Kumar, P., … Zhang, G.-X. (2013). Inhibitory effect of IL-17 on neural stem cell proliferation and neural cell differentiation. *BMC Immunology*, *14*(1), 20. https://doi.org/10.1186/1471-2172-14-20

Lin, F.-M., Pan, Y.-C., Horn, C., Sabbahi, M., & Shenaq, S. (1996). Ankle stance angle: a functional index for the evaluation of sciatic nerve recovery after complete transection. *Journal of Reconstructive Microsurgery*, *12*(3), 173–177.

Lindholm, D., Hengerer, B., Zafra, F., & Thoenen, H. (1990). Transforming growth factor-beta 1 stimulates expression of nerve growth factor in the rat CNA. *Neuroreport*, *1*, 9–12.

Lindholm, D., Heumann, R., Meyer, M., & Thoenen, H. (1987). Interleukin-1 regulates synthesis of nerve growth factor in non-neuronal cells of rat sciatic nerve. *Nature*, *330*(6149), 658–659. https://doi.org/10.1038/330658a0

Lisi, V., Singh, B., Giroux, M., Costigan, M., Woolf, C. J., & Kosik, K. S. (2017). Enhanced Neuronal Regeneration in the CAST/Ei Mouse Strain Is Linked to Expression of Differentiation Markers after Injury. *Cell Reports*, *20*, 1136–1147. https://doi.org/10.1016/j.celrep.2017.07.010

Liu, H., Kim, Y., Chattopadhyay, S., Shubayev, I., Dolkas, J., & Shubayev, V. I. (2010). Matrix metalloproteinase inhibition enhances the rate of nerve regeneration in vivo by promoting dedifferentiation and mitosis of supporting schwann cells. *Journal of Neuropathology and Experimental Neurology*, *69*(4), 386–395. https://doi.org/10.1097/NEN.0b013e3181d68d12

Liu, J.-H., Tang, Q., Liu, X.-X., Qi, J., Zeng, R.-X., Zhu, Z.-W., … Xu, Y.-B. (2018). Analysis of transcriptome sequencing of sciatic nerves in Sprague-Dawley rats of different ages. *Neural Regeneration Research*, *13*(12), 2182–2190. https://doi.org/10.4103/1673-5374.241469

Ma, C. H. E., Omura, T., Cobos, E. J., Latrémolière, A., Ghasemlou, N., Brenner, G. J., … Woolf, C. J. (2011). Accelerating axonal growth promotes motor recovery after peripheral nerve injury in mice. *Journal of Clinical Investigation*, *121*(11), 4332–4347. https://doi.org/10.1172/JCI58675

Mackinnon, S., & Dellon, A. L. (1988). *Surgery of the peripheral nerve*. Theime Medical Publishers.

Maeda, T., Kiguchi, N., Kobayashi, Y., Ikuta, T., Ozaki, M., & Kishioka, S. (2009). Leptin derived from adipocytes in injured peripheral nerves facilitates development of neuropathic pain via macrophage stimulation. *Proceedings of the National Academy of Sciences of the United States of America*, *106*(31), 13076–13081. https://doi.org/10.1073/pnas.0903524106

Olsen, A. S. B., & Færgeman, N. J. (2017). Sphingolipids: Membrane microdomains in brain development, function and neurological diseases. *Open Biology*. Royal Society of London. https://doi.org/10.1098/rsob.170069

Painter, M. W., Brosius Lutz, A., Cheng, Y. C., Latremoliere, A., Duong, K., Miller, C. M., … Woolf, C. J. (2014). Diminished Schwann cell repair responses underlie age-associated

impaired axonal regeneration. *Neuron*, *83*(2), 331–343. https://doi.org/10.1016/j.neuron.2014.06.016

Pestronk, A., Drachman, D. B., & Griffin, J. W. (1980). Effects of aging on nerve sprouting and regeneration. *Experimental Neurology*, *70*(1), 65–82. https://doi.org/10.1016/0014-4886(80)90006-0

Russell, S. A., & Bashaw, G. J. (2018). Axon guidance pathways and the control of gene expression. *Developmental Dynamics*, *247*(4), 571–580. https://doi.org/10.1002/dvdy.24609

Scheib, J., & Höke, A. (2016). Impaired regeneration in aged nerves: Clearing out the old to make way for the new. *Experimental Neurology*, *284*, 79–83. https://doi.org/10.1016/j.expneurol.2016.07.010

Seifert, A. W., Kiama, S. G., Seifert, M. G., Goheen, J. R., Palmer, T. M., & Maden, M. (2012). Skin shedding and tissue regeneration in African spiny mice (Acomys). *Nature*, *489*(7417), 561–565. https://doi.org/10.1038/nature11499

Shepherd, A. J., Mickle, A. D., Golden, J. P., Mack, M. R., Halabi, C. M., De Kloet, A. D., … Mohapatra, D. P. (2018). Macrophage angiotensin II type 2 receptor triggers neuropathic pain. *Proceedings of the National Academy of Sciences of the United States of America*, *115*(34). https://doi.org/10.1073/pnas.1721815115

Sobotka, S., & Mu, L. (2010). Characteristics of tetanic force produced by the sternomastoid muscle of the rat. *Journal of Biomedicine and Biotechnology*. https://doi.org/10.1155/2010/194984

Stratton, J. A., Shah, P. T., Kumar, R., Stykel, M. G., Shapira, Y., Grochmal, J., … Midha, R. (2016). The immunomodulatory properties of adult skin-derived precursor Schwann cells: implications for peripheral nerve injury therapy. *European Journal of Neuroscience*, *43*(3),

365–375. https://doi.org/10.1111/ejn.13006

Surmacz, B., Noisa, P., Risner-Janiczek, J. R., Hui, K., Ungless, M., Cui, W., & Li, M. (2012). DLK1 promotes neurogenesis of human and mouse pluripotent stem cell-derived neural progenitors via modulating notch and BMP signalling. *Stem Cell Reviews and Reports*, *8*(2), 459–471. https://doi.org/10.1007/s12015-011-9298-7

Tanaka, K., & Webster, H. (1991). Myelinated fiber regeneration after crush injury is retarded in sciatic nerves of aging mice. *Journal of Comparative Neurology*, *308*(2), 180–187. https://doi.org/10.1002/cne.903080205

Taskinen, H. S., & Röyttä, M. (1997). The dynamics of macrophage recruitment after nerve transection. *Acta Neuropathologica*, *93*(3), 252–259. https://doi.org/10.1007/s004010050611

Tomlinson, J. E., Žygelytė, E., Grenier, J. K., Edwards, M. G., & Cheetham, J. (2018). Temporal changes in macrophage phenotype after peripheral nerve injury. *Journal of Neuroinflammation*, *15*(185). https://doi.org/10.1186/s12974-018-1219-0

Vaughan, D. W. (1992). Effects of advancing age on peripheral nerve regeneration. *The Journal of Comparative Neurology*, *323*(2), 219–237. https://doi.org/10.1002/cne.903230207

Verdú, E., Ceballos, D., Vilches, J. J., & Navarro, X. (2000). *Influence of aging on peripheral nerve function and regeneration*. *Journal of the Peripheral Nervous System* (Vol. 5).

Wang, Z., Gerstein, M., & Snyder, M. (2009). RNA-Seq: a revolutionary tool for transcriptomics. *Nature Reviews Genetics*, *10*(1), 57–63. https://doi.org/10.1038/nrg2484

Williams, R. R., Venkatesh, I., Pearse, D. D., Udvadia, A. J., & Bunge, M. B. (2015). MASH1/Ascl1a leads to GAP43 expression and axon regeneration in the adult CNS. *PLOS ONE*, *10*(3). https://doi.org/10.1371/journal.pone.0118918

Xing, L., Cheng, Q., Zha, G., & Yi, S. (2017). Transcriptional Profiling at High Temporal Resolution Reveals Robust Immune/Inflammatory Responses during Rat Sciatic Nerve Recovery. *Hindawi*. https://doi.org/10.1155/2017/3827841

Ydens, E., Cauwels, A., Asselbergh, B., Goethals, S., Peeraer, L., Lornet, G., … Janssens, S. (2012). Acute injury in the peripheral nervous system triggers an alternative macrophage response. *Journal of Neuroinflammation*, *9*(1), 176. https://doi.org/10.1186/1742-2094-9-176

Yoshimura, K., Asato, H., Cederna, P. S., Urbanchek, M. G., & Kuzon, W. M. (1999). The effect of reinnervation on force production and power output in skeletal muscle. *Journal of Surgical Research*, *81*(2), 201–208. Retrieved from http://www.idealibrary.com

Yu, P., Matloub, H. S., Sanger, J. R., & Narini, P. (2001). Gait analysis in rats with peripheral nerve injury. *Muscle & Nerve*, *24*(2), 231–239. https://doi.org/10.1002/1097-4598(200102)24:2<231::AID-MUS80>3.0.CO;2-5

Zigmond, R. E., & Echevarria, F. D. (2019). Macrophage biology in the peripheral nervous system after injury. *Progress in Neurobiology*, *173*(December 2018), 102–121. https://doi.org/10.1016/j.pneurobio.2018.12.001